A specialized pore turret in the mammalian cation channel TRPV1 is responsible for distinct and species-specific heat activation thresholds

Received for publication, February 14, 2020, and in revised form, May 20, 2020 Published, Papers in Press, May 27, 2020, DOI 10.1074/jbc.RA120.013037

Guangxu Du[1,‡], Yuhua Tian[1,‡,*], Zhihao Yao[1,2], Simon Vu[3], Jie Zheng[3], Longhui Chai[4], KeWei Wang[1,*], and Shilong Yang[4,*]

From the [1]Department of Pharmacology, Qingdao University School of Pharmacy, Qingdao, Shandong, China, [2]Key Laboratory of Animal Models and Human Disease Mechanisms of the Chinese Academy of Sciences/Key Laboratory of Bioactive Peptides of the Yunnan Province Kunming Institute of Zoology, Kunming, Yunnan, China, [3]University of California Davis, School of Medicine, Davis, California, USA, and [4]College of Wildlife and Protected Area, Northeast Forestry University, Harbin, China

Edited by Mike Shipston

The transient receptor potential vanilloid 1 (TRPV1) channel is a heat-activated cation channel that plays a crucial role in ambient temperature detection and thermal homeostasis. Although several structural features of TRPV1 have been shown to be involved in heat-induced activation of the gating process, the physiological significance of only a few of these key elements has been evaluated in an evolutionary context. Here, using transient expression in HEK293 cells, electrophysiological recordings, and molecular modeling, we show that the pore turret contains both structural and functional determinants that set the heat activation thresholds of distinct TRPV1 orthologs in mammals whose body temperatures fluctuate widely. We found that TRPV1 from the bat *Carollia brevicauda* exhibits a lower threshold temperature of channel activation than does its human ortholog and three bat-specific amino acid substitutions located in the pore turret are sufficient to determine this threshold temperature. Furthermore, the structure of the TRPV1 pore turret appears to be of physiological and evolutionary significance for differentiating the heat-activated threshold among species-specific TRPV1 orthologs. These findings support a role for the TRPV1 pore turret in tuning the heat-activated threshold, and they suggest that its evolution was driven by adaption to specific physiological traits among mammals exposed to variable temperatures.

Accurate detection and response to ambient temperature are of paramount importance for the survival of all organisms living in environments with fluctuating ambient temperatures (1). Both endotherms and ectotherms use cues in ambient temperatures to seek favorable conditions and to avoid harm. Advanced thermoregulatory mechanisms that evolved in endotherms, *e.g.* mammals, further allowed the maintenance of a stable body temperature, which is considered a key factor for the expansion of their livable environment. Due to the distinct habitat temperatures, these animals evolved species-specific temperature-sensing properties that enable them to thrive in diverse environments. Therefore, understanding the molecular bases for these niche properties in different species is important to reveal the underlying mechanisms (2–4).

In most animal species, ambient temperature fluctuation is sensed by peripheral sensory neurons. Thermal sensors expressed in such neurons are key elements to transform temperature changes into electrical signals (5). The transient receptor potential (TRP) vanilloid 1 (TRPV1) ion channel has been identified as a primary heat sensor in mammals (6). TRPV1 is a homotetramer, with each subunit being composed of six transmembrane segments (S1–S6) and long intracellular terminals (7). The central pore of TRPV1 for ion permeation is formed mainly by the P-loop and the S6 segment. The outer pore region, which includes the pore turret, has been suggested to be engaged in temperature-dependent gating and thermal activation processes of TRPV1 or even other temperature-sensitive TRP channels (8–11). Systemic application of capsaicin chemically activates TRPV1, which further leads to thermoregulatory responses, including heat loss and hypothermia (12, 13). Consistently, this thermoregulatory effect of capsaicin is significantly weakened in TRPV1-deficient mice (14). In contrast, antagonists of TRPV1 cause hyperthermia in mammalian species but not in TRPV1-deficient mice (13). Although no discernable difference in core body temperature between TRPV1-deficient and WT mice has been observed, increased vasoconstriction and locomotion activity have been found in these TRPV1-null mice (15). Therefore, TRPV1 plays a crucial role not only in temperature-sensing but also in dynamic regulation of the core body temperature in mammals.

The capacity for thermal homeostasis varies greatly from one species to another, even among mammals. Bats, with a unique body anatomy, exhibit widely fluctuating body temperatures, compared with other mammalian species (Fig. 1*A*). Many known physiological factors, such as mass, basal rate of metabolism, and thermal conductance, affect the variation of animal thermal homeostasis (16, 17). For bats, thermal conductance is extremely high, compared with the body mass, due to the large body surface, which is mainly represented by the thin wings that equip bats for sustained flight (18). Therefore, it is difficult for bats to maintain a steady core temperature with a small body size and a large body surface area. Their body temperature maintains a high level, like that of other mammals, when they

This article contains supporting information.

‡These authors contributed equally to this work.
*For correspondence: Shilong Yang, syang2020@nefu.edu.cn; Yuhua Tian, yhtian05250@qdu.edu.cn; KeWei Wang, wangkw@qdu.edu.cn.

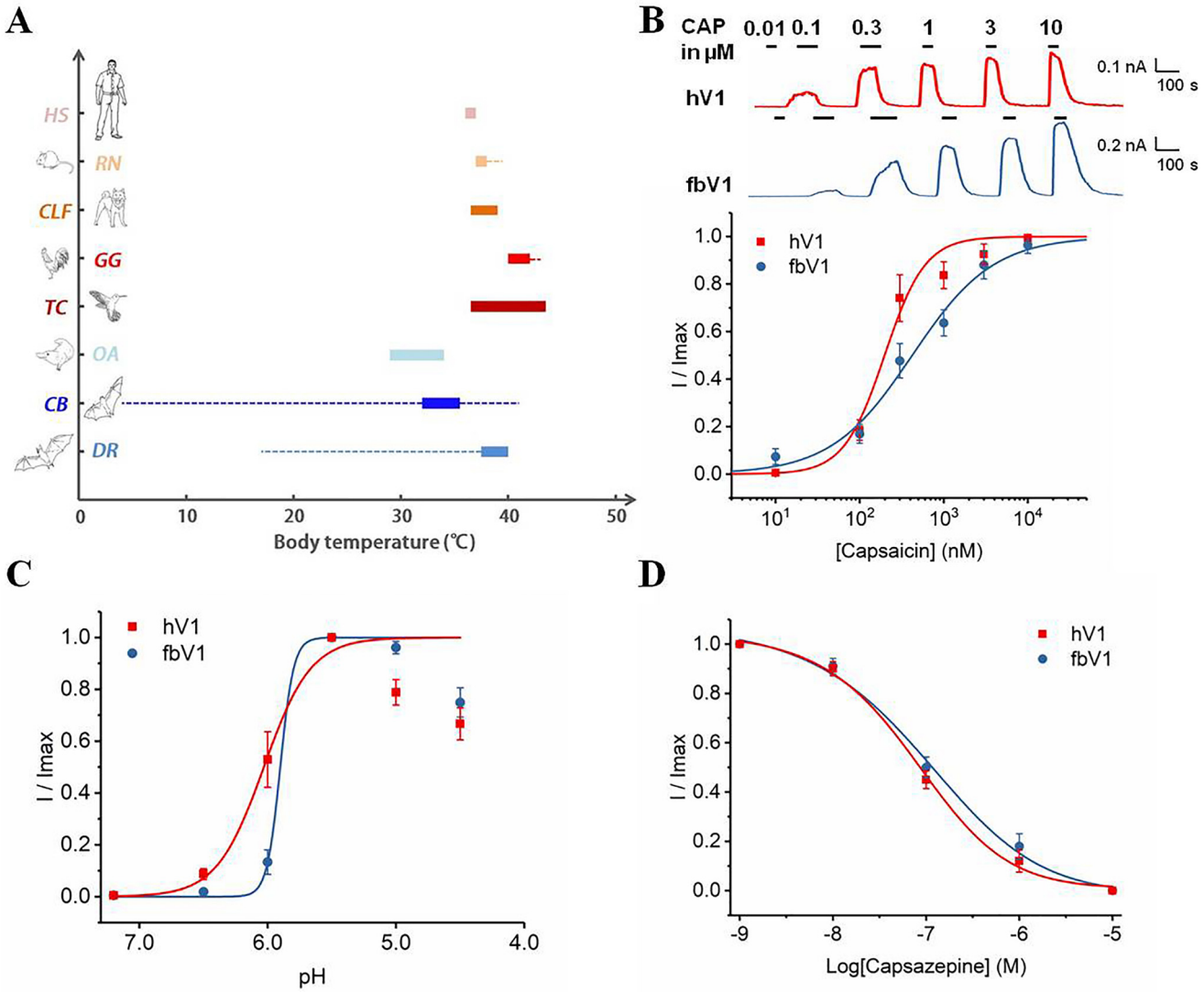

Figure 1. Chemical responses (capsaicin, protons, and capsazepine) of hV1 and fbV1 expressed in HEK293 cells. *A*, diagram illustrating warm-blooded animals' body temperature ranges (*boxes*) and extreme body temperature ranges (*dashed lines*), including human (*HS*, *Homo sapiens*), rat (*RN*, *Rattus norvegicus*), dog (*CLF*, *Canis lupus familiaris*), chicken (*GG*, *Gallus gallus*), hummingbird (*TC*, *Trochilidae*), platypus (*OA*, *Ornithorhynchus anatinus*), fruit bat (*CB*, *Carolia brevicauda*), and vampire bat (*DR*, *Desmodus rotundus*). *B*, representative macroscopic current traces recorded from two WT TRPV1 channels activated by capsaicin (*CAP*) at different concentrations (*top*), and the normalized concentration-response relationships superimposed to fits of a Hill equation (*bottom*). *C*, proton-induced activation of WT channels superimposed to fits of a Hill equation. The data points at higher proton concentrations (pH of ≥5.0) exhibited strong proton inhibition (58) and were excluded from fitting. *D*, capsazepine-induced inhibition of fbV1 and curves representing fits of a Hill equation ($n = 4$ or 5).

fly but drops quickly during resting periods (19). In contrast, humans are capable of maintaining the core body temperature within 1 ℃ (Fig. 1*A*). Given the crucial role of TRPV1 in the thermoregulation of mammals, we first compared the heat activation properties between fruit bat TRPV1 (fbV1) and human TRPV1 (hV1). The lower threshold temperature of fbV1 we found in this study allowed us to further explore the structural determinants for tuning such a threshold value.

Results

Fruit bat TRPV1 with a lower heat activation threshold

We surveyed the literature (4, 20–29) for the normal body temperature range of various homeotherms (Fig. 1*A*). In general, the average body temperature varies widely among animals; however, most animals maintain a rather stable body temperature. Two kinds of bats display a substantially wide range of normal body temperatures (21, 23, 25, 26). Therefore, we synthesized the representative TRPV1 cDNA (GenBank number JN006859.1) of fruit bat (*Carollia brevicauda*) and subcloned it into the eukaryotic expression vector pcDNA3.1 (30). As expected, HEK293 cells expressing fbV1 or its human ortholog hV1 elicited robust channel activation in the presence of known agonists, such as capsaicin (Fig. 1*B* and Table 1) and protons (Fig. 1*C*). In addition, capsaicin-evoked currents of fbV1 were blocked by capsazepine, a prototypical TRPV1 inhibitor (Fig. 1*D*). These results suggest that fbV1 shares similar physical and chemical sensitivities with other mammalian TRPV1 channels.

Given the multiallosteric nature of TRPV1 activation by heat, voltage, and ligands (11), we were able to determine the intrinsic heat activation properties of fbV1 in the absence of other stimuli. To test the heat activation properties, we conducted patch-clamp recording while raising the temperature of the recording chamber. We found that both fbV1 and hV1 channels exhibited

Table 1
Characterization of heat and capsaicin activation of TRPV1 channels and their mutants

TRPV1 type	Temperature threshold (℃)	Q_{10}	EC_{50} (nM)	Hill slope
hV1	42.2 ± 0.5 (n = 5)	10.5 ± 3.5 (n = 5)	197.7 ± 29.0 (n = 4)	1.8 ± 0.4 (n = 4)
fbV1	40.2 ± 0.4 (n = 5)	11.1 ± 3.2 (n = 5)	421.2 ± 59.3 (n = 4)	0.9 ± 0.1 (n = 4)
$V1_{h/fb}$ L	39.7 ± 1.1 (n = 5)	11.8 ± 2.9 (n = 5)	383.9 ± 17.7 (n = 4)	1.4 ± 0.1 (n = 4)
$V1_{h/fb}$ S	40.1 ± 1.2 (n = 5)	12.2 ± 2.4 (n = 5)	198.1 ± 25.5 (n = 3)	1.1 ± 0.1 (n = 3)
$V1_{fb/h}$ L	42.4 ± 0.9 (n = 5)	11.4 ± 3.0 (n = 5)	285.0 ± 48.9 (n = 3)	1.3 ± 0.3 (n = 3)
$V1_{fb/h}$ S	42.0 ± 0.8 (n = 5)	11.1 ± 3.3 (n = 5)	299.3 ± 32.8 (n = 3)	1.3 ± 0.2 (n = 3)
hV1_triple	40.3 ± 0.4 (n = 4)	10.2 ± 2.0 (n = 3)	203.6 ± 14.5 (n = 4)	1.2 ± 0.1 (n = 4)
hP608S	39.7 ± 1.0 (n = 3)	10.8 ± 2.0 (n = 3)	258.2 ± 45.6 (n = 4)	1.5 ± 0.4 (n = 4)
hS613P	43.4 ± 1.0 (n = 3)	11.0 ± 3.0 (n = 3)	108.2 ± 6.8 (n = 3)	2.2 ± 0.4 (n = 3)
hP623S	39.0 ± 2.2 (n = 4)	12.5 ± 2.8 (n = 4)	157.2 ± 20.3 (n = 3)	1.2 ± 0.2 (n = 3)
fbV1_triple	41.9 ± 0.4 (n = 3)	9.4 ± 2.9 (n = 3)	200.2 ± 26.4 (n = 3)	1.8 ± 0.4 (n = 3)
fbS609P	42.3 ± 0.4 (n = 3)	8.8 ± 2.5 (n = 4)	359.5 ± 46.2 (n = 4)	1.0 ± 0.1 (n = 4)
fbP614S	35.0 ± 2.4 (n = 4)	10.2 ± 3.0 (n = 3)	346.7 ± 41.7 (n = 3)	1.2 ± 0.2 (n = 3)
fbS624P	47.5 ± 0.6 (n = 3)	9.3 ± 2.6 (n = 3)	384.1 ± 34.3 (n = 4)	1.0 ± 0.1 (n = 4)

Values are given as mean ± S.D. (n = 3–5).

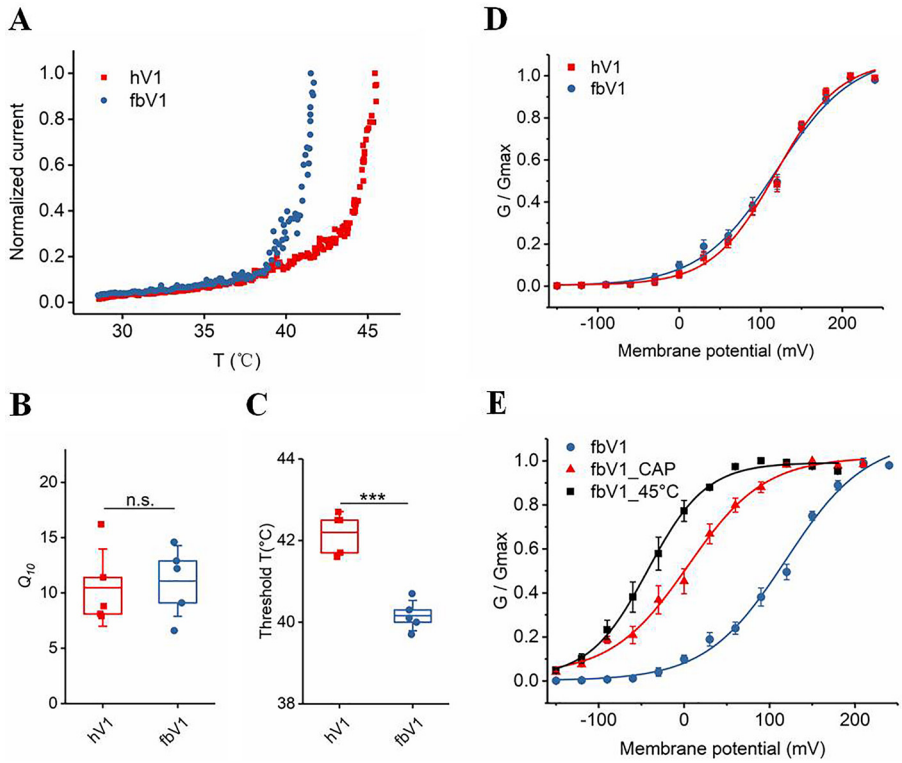

Figure 2. Different heat response profiles of hV1 and fbV1. *A*, example current responses of WT hV1 (*red*) and fbV1 (*blue*) recorded at different temperatures. *B*, the Q_{10} values of hV1 and fbV1 did not show a significant difference. *C*, the thermal threshold for activation of fbV1 is lower than that of hV1. *D*, the conductance-voltage relationships of hV1 and fbV1 were fitted to a Boltzmann function. *E*, heat (45 ℃) and capsaicin (100 nM) shifted the conductance-voltage relationship of fbV1. Data points are fits of a Boltzmann function. The *box top*, *line inside the box*, and *box bottom* represent the 75th percentile, mean, and 25th percentile values, respectively, of each pool of activation temperatures. The *error bars* show the S.D. (n = 5). ***, $p < 0.001$; n.s., no significance, unpaired t test.

robust heat-evoked currents and a steep increase in current amplitude in response to temperature jumps (Fig. 2*A*). Furthermore, we used Q_{10} values (fold increase in current amplitude upon a change in temperature of 10 ℃) to quantify the heat sensitivity, and we found that fbV1 and hV1 showed comparable sensitivity to temperature changes (11.1 ± 3.2 for fbV1 and 10.5 ± 3.5 for hV1) (Fig. 2*B*). Interestingly, we observed that, under our experimental conditions, fbV1 exhibited a temperature activation threshold of 40.2 ± 0.4 ℃, while hV1 showed a threshold of 42.2 ± 0.5 ℃ ($p < 0.001$, n = 5) (Fig. 2*C*). The lower threshold temperature of fbV1 is unlikely to be related to dual allosterism, because fbV1 exhibited an extremely low open probability at +80 mV (Fig. 2*D*). Consistent with TRPV1 behaving as an allosteric protein, we observed an allosteric and nonobligatory coupling of multiple stimuli in fbV1 (Fig. 2*E*). Therefore, these findings demonstrate a significant difference in the threshold temperatures of channel activation, which may be related to the distinct thermoregulation of bats.

Pore turret for tuning the temperature threshold

The discernable difference in the threshold temperature prompted us to explore the structural elements using chimeric constructs between fbV1 and hV1 channels. From the perspective of biophysics, previous studies have suggested that the pore domain of TRPV1 contains the structural elements sufficient for

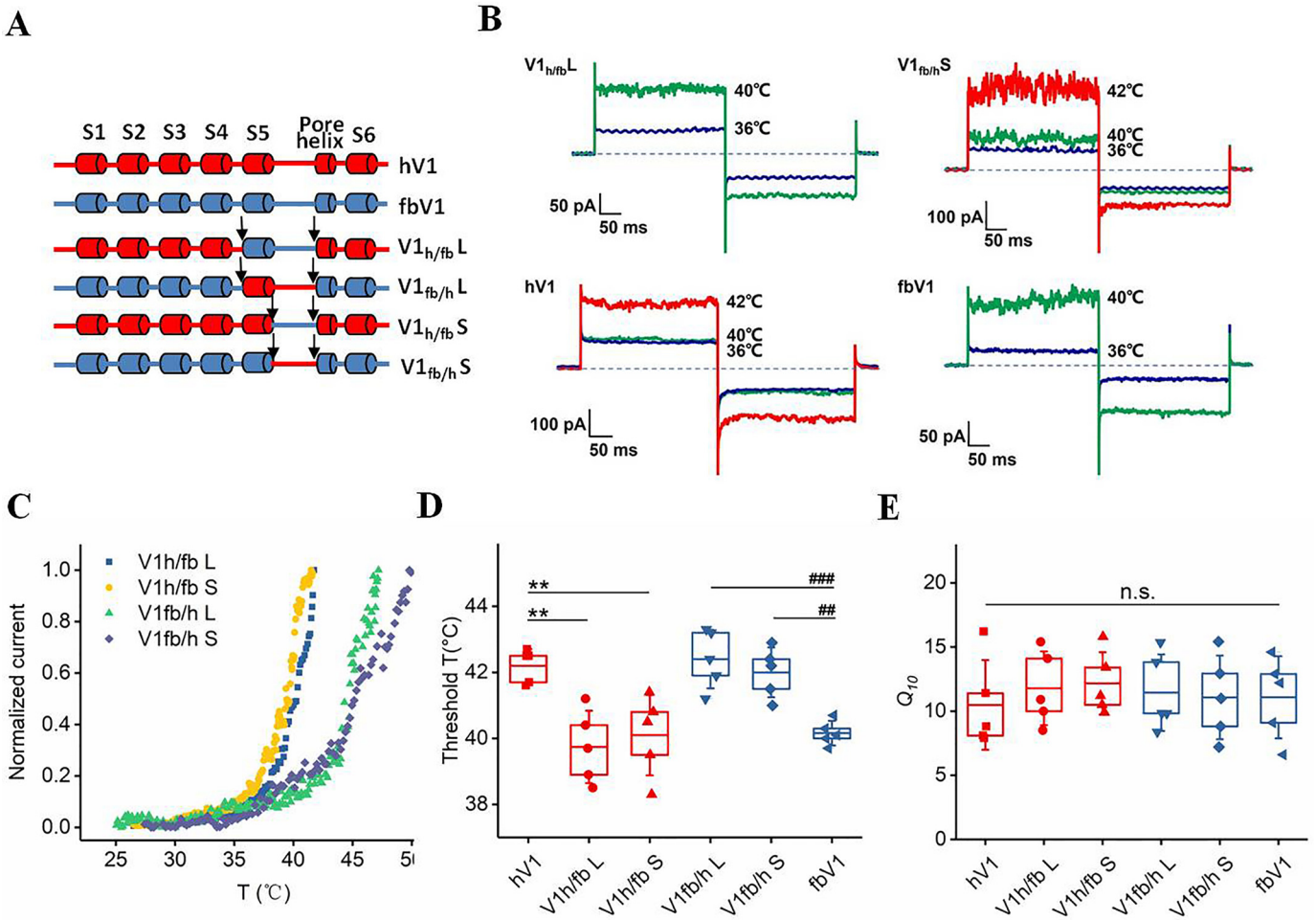

Figure 3. Exchange of the pore turret between hV1 and fbV1 altered their respective original thermal thresholds. *A*, diagram illustrating pore turret exchange between hV1 (*red*) and fbV1 (*blue*). *B*, representative macroscopic current traces recorded from two TRPV1 chimeras and two WT channels activated by heating in the inside-out configuration at stable voltages that pulsed from 0 mV to +80 mV and then from −80 mV to 0 mV. *C*, example current responses of four TRPV1 chimeras recorded at different temperatures. *D*, comparison of Q_{10} values among various WT TRPV1 channels and chimeric channels. *E*, comparison of the thermal threshold for activation among various WT TRPV1 channels and chimeric channels. The *box top*, *line inside the box*, and *box bottom* represent the 75th percentile, mean, and 25th percentile values, respectively, of each pool of activation temperatures. The *error bars* show the S.D. ($n = 5$). **, $p <$ 0.01 *versus* WT hV1; ##, $p < 0.01$; ###, $p < 0.001$ *versus* WT fbV1; n.s., no significance, unpaired *t* test.

heat activation (10, 31–33). As illustrated in Fig. 3*A*, we focused on the pore region by constructing a series of channel chimeras based on fbV1 and hV1. Given that the S6 segments of fbV1 and hV1 are identical in the amino acid sequence, a segment containing either both the S5 segment and the pore turret (labeled L) or just the pore turret (labeled S) was transplanted from fbV1 to hV1, and vice versa. We found that all of the chimeric channels exhibited high sensitivity to capsaicin (Table 1 and Fig. S1) and heat (Fig. 3*B*, Table 1, and Fig. S2) without disruption of the channel function, which allowed us to test the role of the pore regions of fbV1 and hV1 in tuning the threshold temperature. Interestingly, the chimeric channels containing the pore turret of fbV1 ($V1_{h/fb}$ L and $V1_{h/fb}$ S) showed similarly lower threshold temperatures, compared with WT fbV1 (Fig. 3, *C* and *D*). Conversely, the pore turret of hV1 provided the fbV1-based chimeras ($V1_{fb/h}$ L and $V1_{fb/h}$ S) with an elevated threshold temperature similar to that of WT hV1 (Fig. 3, *C* and *D*). In agreement with our observations with WT channels (Fig. 2*B*), these chimeric channels exhibited similar Q_{10} values (11.8 ± 2.9 for $V1_{h/fb}$ L, 11.4 ± 3.0 for $V1f_{b/h}$ L, 12.2 ± 2.4 for $V1_{h/fb}$ S, and 11.1 ± 3.3 for $V1_{fb/h}$ S), indicating that our mutagenesis did not alter the heat sensitivity of these chimeric channels (Fig. 3*E*). Given that the pore turret is sufficient to determine the distinct threshold temperature among the tested TRPV1 channels, the amino acids located in such a motif are likely responsive to these species-specific thresholds for TRPV1 heat activation.

Residue interchange for temperature threshold determination

We focused on the amino acid sequences of the pore turret in fbV1 and hV1. As illustrated in Fig. 4*A*, there are eight non-conserved residues; while many of them are similar in structural and chemical properties, a remarkable interchange between proline and serine at three homologous positions (defined as site 1, site 2, and site 3) is highlighted by the alignment of WT channels. We first mapped them onto structural models of fbV1 and hV1 (Fig. 4*B*), and we observed that all three residues are located in the loop structure, which likely exhibits high thermal flexibility, compared with the transmembrane helices. While this part of the outer pore is predicted to

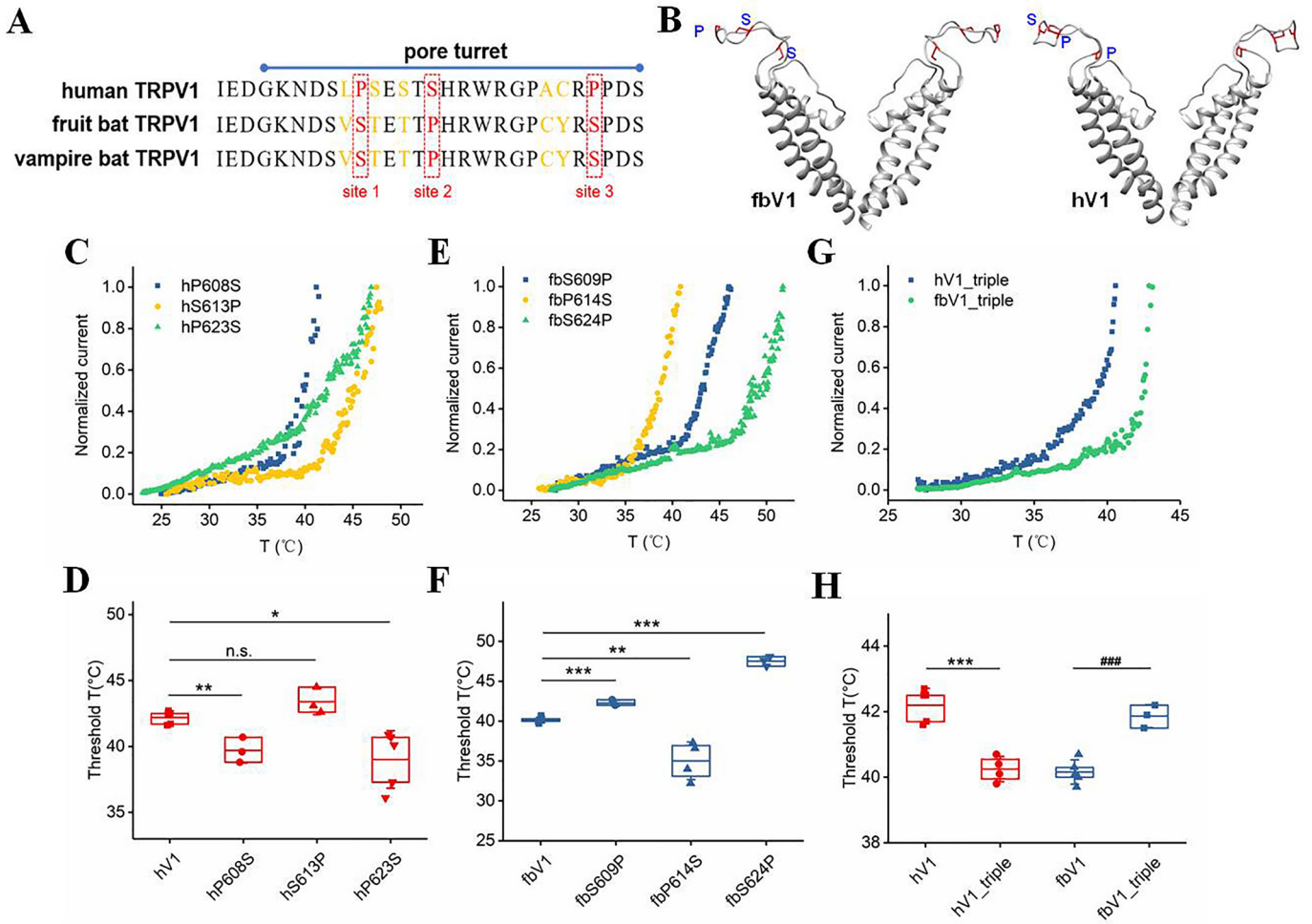

Figure 4. TRPV1 turret interconvertible mutations between hV1 and fbV1 affect their heat responses. *A*, amino acid alignment of hV1, fbV1, and vampire TRPV1 (vbV1) pore turrets. *B*, structural models of the channel pores of hV1 and fbV1, showing the orientations of proline (P) and serine (S) residues located in the pore turret. *C*, current-temperature relationships of three single-point mutant TRPV1 channels based on hV1. *D*, comparison of the thermal thresholds for activation for hV1 and the related single-point mutant channels. *E*, current-temperature relationships of three single-point mutant TRPV1 channels based on fbV1. *F*, comparison of the thermal thresholds for activation for fbV1 and the related single-point mutant channels. *G*, current-temperature relationships of two triple-point mutant TRPV1 channels. *H*, comparison of the thermal thresholds for activation for WT TRPV1 and the triple-point mutant channels. The *box top*, *line inside the box*, and *box bottom* represent the 75th percentile, mean, and 25th percentile values, respectively, of each pool of activation temperatures. The *error bars* show the S.D. (n = 3–5). *, $p < 0.05$; **, $p < 0.01$; ***, $p < 0.001$ versus WT fbV1; ###, $p < 0.001$ versus WT hV1; n.s., no significance, unpaired t test.

have similar overall structures in fbV1 and hV1, the three key residues may take different orientations and hence may experience differences in exposure to the aqueous environment. We set out to test the contribution of such an interchange at each homologous site to the host channel's heat responses. Based on hV1, we found that a single substitution at either site 1 or site 3 dramatically shifted the threshold temperature of the WT channel activation (hP608S for site 1 and hP623S for site 3) (Fig. 4, *C* and *D*, and Fig. S3). Mutation from serine to proline at homologous site 2 in hV1 produced no discernable change in the threshold temperature (Fig. 4, *C* and *D*). Conversely, we mutated these three homologous sites on fbV1 to their corresponding amino acids in hV1. As illustrated in Fig. 4, *E* and *F*, compared with fbV1, substitutions at sites 1 and 3 significantly increased the threshold of heat activation, while the mutation at site 2 caused a decrease in the threshold temperature (fbS609P for site 1, fbP614S for site 2, and fbS624P for site 3). Collectively, these results suggest that such residue interchanges at sites 1–3 are able to independently tune the structural properties of the pore turret, allowing the TRPV1 channel to be activated at different temperatures.

To understand the integrative effect of these sites, we constructed a triple-point mutation based on either hV1 or fbV1 (referred to as hV1_triple and fbV1_triple, respectively). Strikingly, the hV1_triple exhibited a threshold temperature of 40.3 ± 0.4 ℃ (Fig. 4, *G* and *H*), which is very close to that of fbV1. Consistently, the fbV1-based triple-point mutant (fbV1_triple) exhibited an elevated threshold temperature (41.9 ± 0.4 ℃) as high as that of hV1 (Fig. 4, *G* and *H*). All of these channel mutants exhibited similar Q_{10} values (Fig. S4), supporting the conservation of structural integrity and heat sensitivity. Therefore, these findings show that the residue interchange ranging from site 1 to site 3 is sufficient to tune the threshold temperature of TRPV1. More importantly, such substitutions together illustrated that the pore turret participates in setting the species-specific threshold of TRPV1 heat activation, a functional property expected to be crucial in the control of heat loss and the regulation of the bat's body temperature.

Discussion

Identification of the pore turret as a potential module in the thermodynamics of TRP channels (8–11) and other putative protein structures (34–37) can provide insights into the structural basis of temperature sensitivity from a biophysical perspective. Recent studies have suggested that conformational changes of the turret-containing TRPV1 pore domain are required for heat activation (11, 38–40) or even are sufficient to be functionally transplanted with heat activation properties into a temperature-insensitive ion channel (31). Although a single substitution between proline and serine at each of the three sites identified in this study independently alters the threshold temperature of both fbV1 and hV1, it is challenging to speculate, based on the limited data from the present study, whether the effects induced by such mutations are additive. There are at least three possibilities regarding their specific role in tuning TRPV1's threshold temperature, as follows. 1) The contribution of each site to TRPV1 heat activation is totally independent, so that the changed threshold temperature observed with mutations is the result of additive effects of the three sites. 2) As an important apparatus in heat activation, the structure of the TRPV1 pore turret is significantly tuned by these sites with local structural adjustments, allowing both single and triple mutants to exhibit changed threshold temperatures. 3) These substitutions make global changes to the heat-sensitive gating of TRPV1, which is not confined to a specific region of the channel. Indeed, given the significant role of the pore turret in heat activation, it is highly likely that mutations introduced to other turret residues would also affect the heat activation threshold, as previous reports suggested (10, 11). In this sense, our observation that simultaneously swapping three residues switched the heat activation threshold indicates evolutional significance of these residues in shaping the heat-sensing function of the two TRPV1 channels.

From the perspective of temperature-gating mechanisms, the exposed hydrophobic side chains of the amino acids in the pore turret may contribute to such a change in the heat activation threshold in fbV1. At lower temperatures, the hydration shell formed by water molecules surrounding the exposed hydrophobic side chain is expected to be more stable (41), which makes the residues at these three sites energetically favorable in the closed state. Since proline and serine have a significant difference in hydrophobicity (42–44), substitutions at the three sites during evolution may endow fbV1 with unique characteristics during the heat-sensitive gating. Interestingly, the crucial role of hydrophobic side chains has been determined in TRPM8 (45), a prototypical temperature-sensitive TRP channel. Furthermore, proline and serine are different in local structural stability, which may cause a pore turret with such a mutation to undergo distinct temperature-dependent conformational changes at a different temperature. The biological significance of the pore turret in thermoregulatory TRPV1 during evolution has yet to be fully established. In this study, we made the first description of the fbV1 pore turret that shows distinct sequence diversity, which provides this thermoregulator with a lower heat activation threshold in the fruit bat, compared with other mammalian TRPV1 channels. Subjected to widely fluctuating core body temperatures, fbV1 is expected either in the closed state during rest periods or in the open configuration during flying, thus robustly participating in the thermal homeostasis of bats. In this sense, the bat could be an excellent model for understanding the role of TRPV1 in balancing heat generation and loss toward thermal homeostasis.

More generally, the structural elements of mammalian TRPV1 orthologs are found to be flexible in function throughout evolution. Besides the pore turret region, the N and C termini of TRPV1 provide highly evolved mammals with the gating transition for heat-induced desensitization (4). In addition, species-specific N-terminal domains are thought to provide camel and ground squirrel TRPV1 channels with higher heat-activated thresholds (3). Given the crucial role of TRPV1 in ambient temperature detection and thermal homeostasis, we therefore assume that such a fine-tuning molecular mechanism not only is employed by bats, camels, squirrels, and platypuses but also may contribute to the unique thermal adaptation or acclimatization of other mammals with distinct evolutionary drives or special physiological traits.

Including TRPV1, there are a series of molecular thermoregulators used by mammals for delicate thermal homeostasis (46, 47). Given the differences in species-specific ranges of core body temperatures and preferred ambient temperature conditions, the properties (*e.g.* temperature thresholds and sensitivity) of these orthologous thermoregulators are thought to be diverse among species (3, 4, 48–50). Based on our understanding of the bat's TRPV1 pore turret, investigation of the distinct thermal homeostasis in the bat will likely provide another opportunity to reveal biophysical mechanisms of other thermoregulators or even novel functions of thermal detectors.

Experimental Procedures

cDNAs and reagents

WT hV1 and fbV1 were synthesized by TsingKe (Beijing, China). The fused enhanced GFP at the end of the TRPV1 C terminus was used to confirm the protein expression level. The fluorescence tag did not affect the functional properties of the channel, as reported previously (51). Chimeric channels and the mutants were generated by overlapping PCR (fast mutagenesis kit v2) and confirmed by sequencing. Capsaicin and capsazepine were purchased from Abcam (UK) and MedChemExpress (USA), respectively. Lipofectamine 2000 was purchased from Thermo Fisher Scientific (USA).

Transient transfection

HEK293 cells were cultured at 37 ℃ in 5% CO_2 in DMEM with 10% FBS, 100 U/ml penicillin, and 100 mg/ml streptomycin. Cells were transiently transfected with 1.0 μg cDNA using Lipofectamine 2000, according to the manufacturer's instructions. TRPV1-expressing cells were later digested with 0.25% trypsin, between 1 and 2 days after transfection. Electrophysiological experiments were performed after the cells had attached to the glass slide.

Electrophysiological recordings

Macroscopic currents from TRPV1-expressing cells were recorded in the inside-out mode using a HEKA EPC10 amplifier controlled with PatchMaster software (HEKA). Patch pipettes were pulled from thick-walled borosilicate glass (A-M Systems) with a resistance of ~5 MΩ. Both bath and pipette solutions contained 130 mM NaCl, 0.2 mM EDTA, and 3 mM HEPES or MES. For solutions at pH 7.2 to 6.0, HEPES was used as the buffer; for solutions at pH 5.5 to 4.5, MES was used (52). The membrane potential was held at 0 mV, and currents were elicited by a protocol consisting of a 300-ms step to +80 mV followed by a 300-ms step to −80 mV at 1-s intervals. The conductance-voltage curve was determined from currents in response to a series of voltage steps starting from −150 mV. Stimulation of the channels with different concentrations of capsaicin was achieved by perfusion with a rapid solution change system (RSC-200; Biological Science Instruments). Proton-evoked currents were recorded by patch-clamping in the outside-out mode.

Temperature control

Automatic heat control was achieved by using a Warner temperature controller (Model TC-324C). The monitor thermistor of Model CC-28 (Warner Instruments) was placed in the bath to accurately monitor the changes in solution temperature. The HEKA patch-clamp amplifier registered the temperature readout from the thermometer simultaneously with the current recording. The speed of the temperature change was set at a moderate rate of about 0.3 °C/s. This rate ensured that heat-driven gating transitions of the channels reached equilibrium during temperature changes. For testing of ligand-induced channel activation, electrophysiological assays were all conducted at room temperature (~25 °C).

Modeling

Membrane symmetry loop modeling was performed in the Rosetta v3.7 molecular modeling software suite, in which the cryo-EM structure of rat TRPV1 (3J5P) was used as a template. *De novo* modeling of the extracellular pore turret was incorporated using the KIC loop modeling protocol (53). Briefly, around 10,000 models were generated in each round. After seven rounds of loop modeling, the top 10 lowest energy models converged. Once the lowest energy cluster was identified, the transmembrane domains and the extracellular pore turret of mouse TRPV1 and its orthologs were modeled using the comparative modeling application (RosettaCM) (53–57) and subsequently relaxed.

Data analysis

The current-temperature relationship exhibited two phases. The first slow phase represented mostly temperature-dependent increase from the leak current. It was followed by a rapid takeoff phase that represented heat-induced channel activation. A linear fit was conducted for each phase. The intersect point of the two fitting lines was defined as the activation threshold temperature. Q_{10} measurements were used to quantify heat responses here. We first obtained the current amplitude (I_1) at threshold temperature (T_1) from the linear equation of heat activation. The current amplitude (I_2) at a higher temperature ($T_2 = T_1 + 10$ °C) was also obtained from this linear equation, yielding $Q_{10} = (I_2/I_1)^{(10/(T_2 - T_1))}$. The capsaicin concentration dependence of the current amplitude was fitted to a Hill equation to estimate the EC_{50} and slope factor values, using IGOR PRO software (WaveMetrics). Data points for chemically induced activation or inhibition were fitted to a Hill equation. The plots for the conductance-voltage relationship were fitted to a Boltzmann function. All statistical values are shown as means ± S.D., and the n value represents the sample size of the experiment. Statistical analysis was performed using unpaired Student's t tests.

Data availability

All data are contained within the manuscript.

Acknowledgments—We are grateful to our laboratory members for assistance and discussion and to Fan Yang and Xiancui Lu for advice on data analysis.

Author contributions—G. D., Y. T., Z. Y., S. V., and J. Z. formal analysis; G. D. and Y. T. methodology; G. D., Y. T., L. C., and S. Y. writing-original draft; Z. Y., S. V., J. Z., L. C., K. W., and S. Y. conceptualization; Z. Y., S. V., J. Z., L. C., K. W., and S. Y. supervision; Z. Y., S. V., L. C., K. W., and S. Y. investigation; Z. Y., S. V., J. Z., L. C., K. W., and S. Y. writing-review and editing; L. C. and S. Y. funding acquisition.

Funding and additional information—This work was supported by funding from the National Science Foundation of China, Grants 31640071 and 3177083 (to S. Y.) and from the National Institutes of Health Grant R01NS072377 (to J. Z.). The content is solely the responsibility of the authors and does not necessarily represent the official views of the National Institutes of Health.

Conflict of interest—The authors declare that they have no conflicts of interest with the contents of this article.

Abbreviations—The abbreviations used are: TRP, transient receptor potential; TRPV1, transient receptor potential vanilloid 1; fbV1, fruit bat transient receptor potential vanilloid 1; hV1, human transient receptor potential vanilloid 1.

References

1. Boron, W. F., and Boulpaep, E. L. (2016) *Medical Physiology eBook*, 3rd Ed., Elsevier Health Sciences, Philadelphia, PA
2. Matos-Cruz, V., Schneider, E. R., Mastrotto, M., Merriman, D. K., Bagriantsev, S. N., and Gracheva, E. O. (2017) Molecular prerequisites for diminished cold sensitivity in ground squirrels and hamsters. *Cell Rep.* **21,** 3329–3337 CrossRef Medline
3. Laursen, W. J., Schneider, E. R., Merriman, D. K., Bagriantsev, S. N., and Gracheva, E. O. (2016) Low-cost functional plasticity of TRPV1 supports heat tolerance in squirrels and camels. *Proc. Natl. Acad. Sci. U.S.A.* **113,** 11342–11347 CrossRef Medline

4. Luo, L., Wang, Y., Li, B., Xu, L., Kamau, P. M., Zheng, J., Yang, F., Yang, S., and Lai, R. (2019) Molecular basis for heat desensitization of TRPV1 ion channels. *Nat. Commun.* **10,** 2134 CrossRef Medline
5. Patapoutian, A., Peier, A. M., Story, G. M., and Viswanath, V. (2003) ThermoTRP channels and beyond: mechanisms of temperature sensation. *Nat. Rev. Neurosci.* **4,** 529–539 CrossRef Medline
6. Caterina, M. J., Schumacher, M. A., Tominaga, M., Rosen, T. A., Levine, J. D., and Julius, D. (1997) The capsaicin receptor: a heat-activated ion channel in the pain pathway. *Nature* **389,** 816–824 CrossRef Medline
7. Liao, M., Cao, E., Julius, D., and Cheng, Y. (2013) Structure of the TRPV1 ion channel determined by electron cryo-microscopy. *Nature* **504,** 107–112 CrossRef Medline
8. Grandl, J., Hu, H., Bandell, M., Bursulaya, B., Schmidt, M., Petrus, M., and Patapoutian, A. (2008) Pore region of TRPV3 ion channel is specifically required for heat activation. *Nat. Neurosci.* **11,** 1007–1013 CrossRef Medline
9. Myers, B. R., Bohlen, C. J., and Julius, D. (2008) A yeast genetic screen reveals a critical role for the pore helix domain in TRP channel gating. *Neuron* **58,** 362–373 CrossRef Medline
10. Cui, Y., Yang, F., Cao, X., Yarov-Yarovoy, V., Wang, K., and Zheng, J. (2012) Selective disruption of high sensitivity heat activation but not capsaicin activation of TRPV1 channels by pore turret mutations. *J. Gen. Physiol.* **139,** 273–283 CrossRef Medline
11. Yang, F., Cui, Y., Wang, K., and Zheng, J. (2010) Thermosensitive TRP channel pore turret is part of the temperature activation pathway. *Proc. Natl. Acad. Sci. U.S.A.* **107,** 7083–7088 CrossRef Medline
12. Wang, H., and Siemens, J. (2015) TRP ion channels in thermosensation, thermoregulation and metabolism. *Temperature (Austin)* **2,** 178–187 CrossRef Medline
13. Gavva, N. R., Treanor, J. J. S., Garami, A., Fang, L., Surapaneni, S., Akrami, A., Alvarez, F., Bak, A., Darling, M., Gore, A., Jang, G. R., Kesslak, J. P., Ni, L., Norman, M. H., Palluconi, G., *et al.* (2008) Pharmacological blockade of the vanilloid receptor TRPV1 elicits marked hyperthermia in humans. *Pain* **136,** 202–210 CrossRef Medline
14. Caterina, M. J., Leffler, A., Malmberg, A. B., Martin, W. J., Trafton, J., Petersen-Zeitz, K. R., Koltzenburg, M., Basbaum, A. I., and Julius, D. (2000) Impaired nociception and pain sensation in mice lacking the capsaicin receptor. *Science* **288,** 306–313 CrossRef Medline
15. Garami, A., Pakai, E., Oliveira, D. L., Steiner, A. A., Wanner, S. P., Almeida, M. C., Lesnikov, V. A., Gavva, N. R., and Romanovsky, A. A. (2011) Thermoregulatory phenotype of the Trpv1 knockout mouse: thermoeffector dysbalance with hyperkinesis. *J. Neurosci.* **31,** 1721–1733 CrossRef Medline
16. McNab, B. K. (1966) The metabolism of fossorial rodents: a study of convergence. *Ecology* **47,** 712–733 CrossRef
17. McNab, B. K. (1970) Body weight and the energetics of temperature regulation. *J. Exp. Biol.* **53,** 329–348 Medline
18. Hunter, P. (2007) The nature of flight: the molecules and mechanics of flight in animals. *EMBO Rep.* **8,** 811–813 CrossRef Medline
19. Kluger, M. J., and Heath, J. E. (1970) Vasomotion in the bat wing: a thermoregulatory response to internal heating. *Comp. Biochem. Physiol.* **32,** 219–226 CrossRef Medline
20. Brown, J. W., and Pham-Le, N. M. (2012) The effect of thermopreference on circadian thermoregulation in Sprague-Dawley and Fisher 344 rats. *J. Therm. Biol.* **37,** 309–315 CrossRef
21. Lyman, C. P., and Wimsatt, W. A. (1966) Temperature regulation in the vampire bat, *Desmodus rotundus*. *Physiol. Zool.* **39,** 101–109 CrossRef
22. Ketz-Riley, C. J., and Sanchez, C. R. (2015) Chapter 26: Trochiliformes (hummingbirds). in *Fowler's Zoo and Wild Animal Medicine* (Miller, R. E., and Fowler, M. E., eds.), Vol. 8, pp. 209–213, W.B. Saunders, St. Louis, MO
23. Bonaccorso, F. J., and McNab, B. K. (1997) Plasticity of energetics in blossom bats (Pteropodidae): impact on distribution. *J. Mammal.* **78,** 1073–1088 CrossRef
24. Yang, Y., Zhen, C., Yang, B., Yu, Y., and Pan, J. (2018) The effect of 580 nm-based-LED mixed light on growth, adipose deposition, skeletal development, and body temperature of chickens. *J. Photochem. Photobiol. B Biol.* **183,** 288–292 CrossRef Medline
25. McNab, B. K. (1989) Temperature regulation and rate of metabolism in three Bornean bats. *J. Mammal.* **70,** 153–161 CrossRef
26. Studier, E. H., and Wilson, D. E. (1970) Thermoregulation in some neotropical bats. *Comp. Biochem. Physiol.* **34,** 251–262 CrossRef Medline
27. Hall, E. J., and Carter, A. (2017) Establishing a reference range for normal canine tympanic membrane temperature measured with a veterinary aural thermometer. *Vet. Nurs. J.* **32,** 369–373 CrossRef
28. Kuht, J., and Farmery, A. D. (2018) Body temperature and its regulation. *Anaesth. Intensive Care Med.* **19,** 507–512 CrossRef
29. Holz, P. (2015) Chapter 32: Monotremata (Echidna, Platypus). in *Fowler's Zoo and Wild Animal Medicine* (Miller, R. E., and Fowler, M. E., eds.), Vol. 8, pp. 247–255, W.B. Saunders, St. Louis, MO.
30. Han, Y., Li, B., Yin, T.-T., Xu, C., Ombati, R., Luo, L., Xia, Y., Xu, L., Zheng, J., Zhang, Y., Yang, F., Wang, G.-D., Yang, S., and Lai, R. (2018) Molecular mechanism of the tree shrew's insensitivity to spiciness. *PLoS Biol.* **16,** e2004921 CrossRef Medline
31. Zhang, F., Jara-Oseguera, A., Chang, T. H., Bae, C., Hanson, S. M., and Swartz, K. J. (2018) Heat activation is intrinsic to the pore domain of TRPV1. *Proc. Natl. Acad. Sci. U.S.A.* **115,** e317–e324 CrossRef Medline
32. Ma, L., Yang, F., Vu, S., and Zheng, J. (2016) Exploring functional roles of TRPV1 intracellular domains with unstructured peptide-insertion screening. *Sci. Rep.* **6,** 33827 CrossRef Medline
33. Yang, F., and Zheng, J. (2014) High temperature sensitivity is intrinsic to voltage-gated potassium channels. *Elife* **3,** e03255 CrossRef Medline
34. Yao, J., Liu, B., and Qin, F. (2011) Modular thermal sensors in temperature-gated transient receptor potential (TRP) channels. *Proc. Natl. Acad. Sci. U.S.A.* **108,** 11109–11114 CrossRef Medline
35. Zheng, W., and Wen, H. (2019) Heat activation mechanism of TRPV1: new insights from molecular dynamics simulation. *Temperature (Austin)* **6,** 120–131 CrossRef Medline
36. Sosa-Pagan, J. O., Iversen, E. S., and Grandl, J. (2017) TRPV1 temperature activation is specifically sensitive to strong decreases in amino acid hydrophobicity. *Sci. Rep.* **7,** 549 CrossRef Medline
37. Ladrón-de-Guevara, E., Dominguez, L., Rangel-Yescas, G. E., Fernández-Velasco, D. A., Torres-Larios, A., Rosenbaum, T., and Islas, L. D. (2020) The contribution of the ankyrin repeat domain of TRPV1 as a thermal module. *Biophys. J.* **118,** 836–845 CrossRef Medline
38. Yang, S., Yang, F., Wei, N., Hong, J., Li, B., Luo, L., Rong, M., Yarov-Yarovoy, V., Zheng, J., Wang, K., and Lai, R. (2015) A pain-inducing centipede toxin targets the heat activation machinery of nociceptor TRPV1. *Nat. Commun.* **6,** 8297 CrossRef Medline
39. Cao, X., Ma, L., Yang, F., Wang, K., and Zheng, J. (2014) Divalent cations potentiate TRPV1 channel by lowering the heat activation threshold. *J. Gen. Physiol.* **143,** 75–90 CrossRef Medline
40. Yang, F., Ma, L., Cao, X., Wang, K., and Zheng, J. (2014) Divalent cations activate TRPV1 through promoting conformational change of the extracellular region. *J. Gen. Physiol.* **143,** 91–103 CrossRef Medline
41. Chowdhury, S., Jarecki, B. W., and Chanda, B. (2014) A molecular framework for temperature-dependent gating of ion channels. *Cell* **158,** 1148–1158 CrossRef Medline
42. Hessa, T., Kim, H., Bihlmaier, K., Lundin, C., Boekel, J., Andersson, H., Nilsson, I., White, S. H., and von Heijne, G. (2005) Recognition of transmembrane helices by the endoplasmic reticulum translocon. *Nature* **433,** 377–381 CrossRef Medline
43. Moon, C. P., and Fleming, K. G. (2011) Side-chain hydrophobicity scale derived from transmembrane protein folding into lipid bilayers. *Proc. Natl. Acad. Sci. U.S.A.* **108,** 10174–10177 CrossRef Medline
44. Zhu, C., Gao, Y., Li, H., Meng, S., Li, L., Francisco, J. S., and Zeng, X. C. (2016) Characterizing hydrophobicity of amino acid side chains in a protein environment via measuring contact angle of a water nanodroplet on planar peptide network. *Proc. Natl. Acad. Sci. U.S.A.* **113,** 12946–12951 CrossRef Medline
45. Yang, S., Lu, X., Wang, Y., Xu, L., Chen, X., Yang, F., and Lai, R. (2020) A paradigm of thermal adaptation in penguins and elephants by tuning cold activation in TRPM8. *Proc. Natl. Acad. Sci. U.S.A.* **117,** 8633–8638 CrossRef
46. Tan, C. L., and Knight, Z. A. (2018) Regulation of body temperature by the nervous system. *Neuron* **98,** 31–48 CrossRef Medline
47. Bagriantsev, S. N., and Gracheva, E. O. (2015) Molecular mechanisms of temperature adaptation. *J. Physiol.* **593,** 3483–3491 CrossRef Medline

48. Gracheva, E. O., Cordero-Morales, J. F., González-Carcacía, J. A., Ingolia, N. T., Manno, C., Aranguren, C. I., Weissman, J. S., and Julius, D. (2011) Ganglion-specific splicing of TRPV1 underlies infrared sensation in vampire bats. *Nature* **476,** 88–91 CrossRef Medline
49. Gracheva, E. O., and Bagriantsev, S. N. (2015) Evolutionary adaptation to thermosensation. *Curr. Opin. Neurobiol.* **34,** 67–73 CrossRef Medline
50. Papakosta, M., Dalle, C., Haythornthwaite, A., Cao, L., Stevens, E. B., Burgess, G., Russell, R., Cox, P. J., Phillips, S. C., and Grimm, C. (2011) The chimeric approach reveals that differences in the TRPV1 pore domain determine species-specific sensitivity to block of heat activation. *J. Biol. Chem.* **286,** 39663–39672 CrossRef Medline
51. Cheng, W., Yang, F., Takanishi, C. L., and Zheng, J. (2007) Thermosensitive TRPV channel subunits coassemble into heteromeric channels with intermediate conductance and gating properties. *J. Gen. Physiol.* **129,** 191–207 CrossRef Medline
52. Yang, S., Yang, F., Zhang, B., Lee, B. H., Li, B., Luo, L., Zheng, J., and Lai, R. (2017) A bimodal activation mechanism underlies scorpion toxin-induced pain. *Sci. Adv.* **3,** e1700810 CrossRef Medline
53. Qian, B., Raman, S., Das, R., Bradley, P., McCoy, A. J., Read, R. J., and Baker, D. (2007) High-resolution structure prediction and the crystallographic phase problem. *Nature* **450,** 259–264 CrossRef Medline
54. Meiler, J., and Baker, D. (2006) RosettaLigand: protein-small molecule docking with full side-chain flexibility. *Proteins* **65,** 538–548 CrossRef Medline
55. Bender, B. J., Cisneros, A., III, Duran, A. M., Finn, J. A., Fu, D., Lokits, A. D., Mueller, B. K., Sangha, A. K., Sauer, M. F., Sevy, A. M., Sliwoski, G., Sheehan, J. H., DiMaio, F., Meiler, J., and Moretti, R. (2016) Protocols for molecular modeling with Rosetta3 and RosettaScripts. *Biochemistry* **55,** 4748–4763 CrossRef Medline
56. Davis, I. W., and Baker, D. (2009) RosettaLigand docking with full ligand and receptor flexibility. *J. Mol. Biol.* **385,** 381–392 CrossRef Medline
57. Davis, I. W., Raha, K., Head, M. S., and Baker, D. (2009) Blind docking of pharmaceutically relevant compounds using RosettaLigand. *Protein Sci.* **18,** 1998–2002 CrossRef Medline
58. Lee, B. H., and Zheng, J. (2015) Proton block of proton-activated TRPV1 current. *J. Gen. Physiol.* **146,** 147–159 CrossRef Medline